

Synthesis and Characterization of Poly(1,3-dioxolane) Using Green Catalyst. Application as Superplasticizer or Dispersant in Cement Paste

Assia Belarbi^{a,b,*}, Nora Ouis^a, Larbi Kacimi^b, and Nassira Benharrats^a

^a *Laboratoire de Physique des Plasmas, Matériaux Conducteur et leurs Applications, Faculté de Chimie, Université des Sciences et de la Technologie d'Oran-Mohamed Boudiaf, El M'naouer, USTO, Oran, B.P. 1505 Algérie*

^b *Laboratoire des Eco-Matériaux Fonctionnels et Nanostructurés, Faculté de Chimie, Université des Sciences et de la Technologie d'Oran-Mohamed Boudiaf, El M'Naouer, USTO, Oran, B.P. 1505 Algérie*

*e-mail: belarbi.assia@yahoo.fr; assia.belarbi@univ-usto.dz

Received December 21, 2023; revised May 13, 2024; accepted May 21, 2024

Abstract—1,3-Dioxolane polymer (PDXL) was synthesized using Halloysite, a natural clay material, as solid acid catalyst for cationic ring-opening polymerization. This catalyst was activated with 0.5 M sulfuric acid solution to increase its Brønsted-type acidity. Polymerization of DXL was carried out in bulk under magnetic stirring at low temperature, leading to the formation of polydioxolane. The Halloysite and synthesized polymer were characterized by several techniques including X-ray fluorescence (XRF), X-ray diffraction (XRD), Infrared spectroscopy (FTIR), and nuclear magnetic resonance (NMR). To assess the dispersing power of the synthesized PDXL and its hydration activity, the setting time, consistence and compressive strength of cement paste and mortar containing poly(1,3-dioxolane) was studied, compared to the commercial polyethylene glycol (PEG) used as reference in this study. The results showed the retarding effect of PDXL on the setting times of cement paste, accompanied by a decrease in normal consistency, which allows its use as superplasticizer or dispersant agent. Thus, PDXL improved the compressive strength of cement mortar compared to PEG polymer effect.

DOI: 10.1134/S156009042460102X

INTRODUCTION

Polydioxolane (PDXL) is a water-soluble linear synthetic polymer obtained from dioxolane monomer. Such as polyethylene glycol (PEG), which is widely used in many research areas (biomedical and construction fields) [1, 2], PDXL is a polymer with large application potential. To improve its physicochemical properties for different applications, PDXL can be functionalized solely by end-chain hydroxyl groups because its polymer skeleton does not contain reactive groups [3].

Cationic polymerization is a synthesis method usually used for preparing polymers by various homogeneous initiators (Lewis acids). Nevertheless, these initiators are characterized by their high toxicity and their very difficult separation from polymer product. The last decade, many studies were conducted to replace these initiators by new non-toxic heterogeneous catalysts. Among these catalysts, clay minerals (montmorillonite and kaolin) were used in several polymerization and copolymerization reactions of vinylic and heterocyclic monomers [4–8].

Halloysite (HAL) is a phyllosilicate 1 : 1 aluminosilicate clay mineral of the kaolin group, with chemical for-

mula $\text{Al}_2\text{Si}_2\text{O}_5(\text{OH})_4 \cdot n\text{H}_2\text{O}$. It is distinguished from kaolin by its intercalated water content and its tubular structure. Halloysite is used in several fields like dyes and heavy metals absorption [9–12], heterogeneous catalysis in esterification reactions [13], biocomposites for biomedical applications [14, 15] and nanocomposite coatings for potential industrial applications [16].

In this work, halloysite was treated with sulfuric acid to promote its acid sites and remove the mineral impurities. The treatment was conducted softly and carefully in order to preserve the halloysite structure. Acid-activated halloysite was used as an eco-catalyst to synthesize poly(1,3-dioxolane) (PDXL) via cationic ring-opening polymerization of 1,3-dioxolane. 1,3-Dioxolane (DXL) is an heterocyclic monomer containing acetal function, favorable for cationic polymerization [17].

The last two decades, PDXL was used as macromonomer to prepare hydrogel compounds [18, 19], but no use as superplasticizer in the cement paste rheology area is known. Polydioxolane is characterized by uncomplicated chemical structure compared to traditional superplasticizers, such as naphthalene series

Table 1. Chemical compositions (wt %) and Physical properties of the used cement (CEM I)

Oxides	SiO ₂	Al ₂ O ₃	CaO	Fe ₂ O ₃	MgO	SO ₃	K ₂ O	Na ₂ O	f-CaO
wt %	19.70	4.54	64.30	2.98	3.64	2.19	0.70	0.2	1.02
Physical properties			Blaine specific surface area, cm ² /g				Density, g/cm ³		
Measured values			4040				3.1		

(NPS) [20] and polycarboxylate (PC) superplasticizers [21], having very complex molecular structures. Superplasticizers, used as dispersant additives in cement paste, are frequently grafted copolymers or terpolymers consisting of two or three different monomers.

Polydioxolane is a homopolymer, which can be easily synthesized by cationic polymerization method. Its high water affinity promotes its mixing with different cement hydrates during hydration process. In this work, PDXL was synthesized and used as superplasticizer in cement paste while studying its effect on cement setting. The industrial polyethylene glycol (PEG) was used as control sample in this study. PEG has been widely used as superplasticizer in concrete due to its outstanding properties compared to traditional polyelectrolyte dispersants, resulting from its grafting as a side chain onto the linear chain of comb-shaped copolymer [22].

The main objectives of this study are the valorization of an Algerian halloysite in heterogeneous catalysis for polymerization reactions, and the use of halloysite-based synthesized polydioxolane as dispersing additive in cement suspension during hydration process. PDXL could be an economic alternative for cement paste superplasticizer.

EXPERIMENTAL

Reactive Products

1,3-Dioxolane (DXL) (BIOCHEM, 99%), sulfuric acid (BIOCHEM, 98%), dichloromethane (DCM) (Sigma Aldrich, 99%), hexane (BIOCHEM, 99%), silver nitrate (BIOCHEM, 99%) and poly(ethylene glycol) (PEG) (PROLABO, 99%) were used to synthesize poly(1,3-dioxolane) polymer (PDXL). The used Halloysite is an Algerian clay from the Djebel Debagh deposit, located in the north-east of Algeria. Portland cement (CEM I), used for testing the polymer effect on its setting time, was obtained from Lafarge plant of Oggaz, Algeria. Its chemical composition and physical properties (density and Blaine specific area) are shown in Table 1.

Characterization Methods

The specific surface area of samples, determined by Brunauer Emmett Teller method (BET), was measured by Nitrogen sorption at 77 K using 3Flex V5.00 from Micromeritics. The chemical analysis of the clay

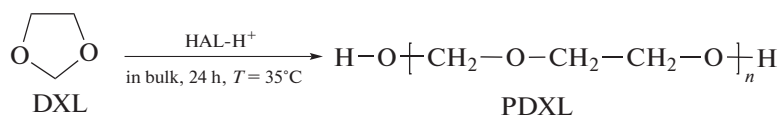
material was obtained by X-ray fluorescence (FRX) using Philips Magix-Pro equipment. The X-ray diffraction (XRD) patterns of the samples were carried out with a Rigaku Miniflex 300/600 powder X-ray diffractometer using CuK_α radiation ($\lambda = 1.5406 \text{ \AA}$), in 2θ angle range from 5° to 70° , with a scanning speed of $5^\circ/\text{min}$, operated at 40 kV and 15 mA. The obtained samples were characterized by infrared (FTIR) spectroscopy using Bruker Alpha-OPUS spectrometer with ATR cell in the region of $4000\text{--}500 \text{ cm}^{-1}$. The Nuclear Magnetic Resonance spectra were recorded on a Bruker-Ascend 300 MHz apparatus in deuterated dimethyl sulfoxide (DMSO-d₆). The setting time and standard consistency of cement paste were determined by Vicat apparatus, according to NF EN 196-3 standard.

Cement with water were mixed for 90 min in a mixer at moderate speed. The obtained cement paste was quickly introduced into Vicat mold.

The initial setting time is measured when the needle is at $4 \pm 1 \text{ mm}$ from the mold bottom, while the final setting time is obtained when the Vicat needle penetrates 0.5 mm into the cement paste. The normal consistency is obtained when the probe vertically penetrates the center of the cement paste at $6 \pm 1 \text{ mm}$ from the lower edge of the paste surface (NF EN 196-3). The compressive strength was measured according to NF EN 196-1 standard, of which standard mortar specimens ($4 \times 4 \times 16 \text{ cm}^3$) at room temperature were prepared with water/cement and cement/sand mass ratios of 0.5 and 1/3, respectively. The standardized sand was added to the cement paste and mixed at high speed. The mixture (mortar) is filled into the mold (consisting of 3 specimens) and placed on the vibration table for 120 s. After 24 hours in a humidity chamber, the specimens were demolded and stored in a water bath at $20 \pm 1^\circ\text{C}$.

Synthesis Procedure

The synthesis process was divided into two stages: the first stage was the preparation of the acidified halloysite (HAL-H⁺) for using it as catalyst in the polymer synthesis. A purified halloysite (10 g) was dispersed in 500 mL of sulfuric acid solution (0.5 M) and stirred at room temperature for 48 h using a magnetic stirring plate of 3500 tr/min. The halloysite suspension was separated by centrifugation process and washed with demineralized water until the chlorides test with



Scheme 1.

AgNO₃ solution is negative. The obtained clay was then dried, crushed and stored in a desiccator. The second stage was the synthesis of poly (1, 3-dioxolane) (PDXL) with HAL-H⁺ as catalyst. This polymer was obtained using the ring opening cationic polymerization method, of which 5 g (0.0675 mmol) of 1, 3-dioxolane was placed in 100 mL flask equipped with a condenser, and then the acidified halloysite clay (HAL-H⁺) was added with mass percentage of 10%. The chemical reaction (Scheme 1) was kept under magnetic stirring for 24 hours at 35°C, before the separation of the clay by filtration. The polymer was dissolved in dichloromethane and then collected by precipitation in hexane. The reaction yield was estimated at 71.4%.

RESULTS AND DISCUSSION

Characterizations of HAL and HAL-H⁺

Physical and chemical properties of HAL. The specific surface area of the halloysite (HAL), determined by BET method, was 59.96 m²/g. This value was higher than that of kaolin used as a catalyst in polymer synthesis [23]. The chemical composition of halloysite (Table 2), determined by FRX analysis, shows that this clay is mainly composed from silica and alumina in addition to low amount of calcium oxide, with SiO₂/Al₂O₃ mass ratio equal to 1.17. A high ignition loss was observed due to the great presence of chemical bonded water of clay minerals.

X-ray diffraction (XRD) characterization. The X-ray diffractograms of the natural halloysite (HAL) and its acid-activated form (HAL-H⁺) are presented in Fig. 1.

The XRD patterns of the natural halloysite (Fig. 1, curve 1) show two peaks at 8.96°/2θ (*d*₀₀₁ = 9.861 Å) and 12.11°/2θ (*d*₀₀₁ = 7.302 Å) corresponding to 10Å-halloysite and 7Å-halloysite, respectively [24]. The 10 Å-halloysite is easily transformed into 7Å-halloysite by partial dehydration under ambient temperature and humidity or by moderate heating [25]. Its heating to 200°C will transform it completely into

dehydrated form [24]. The reflections (002) (*d*₀₀₂ = 3.541 Å) at 25.12°/2θ, (123) (*d*₁₂₃ = 1.89 Å) at 47.99°/2θ, (114) (*d*₁₁₄ = 1.67 Å) at 54.86°/2θ, corresponding to halloysite mineral [26], are also indexed (Fig. 1, curve 1). The (020) reflection of 4.391 Å at 20.20°/2θ is characteristic to the tubular morphology of halloysite. The peaks at 35.46°/2θ (*d*₁₂₂ = 2.53 Å), 39.68°/2θ (*d*₁₃₁ = 2.27 Å), 60.26°/2θ (*d*₁₅₂ = 1.53 Å), 62.77°/2θ (*d*₃₃₁ = 1.48 Å) characterize the presence of few amount of kaolinite, with trace of feldspar at 27.87°/2θ (*d*₁₁₀ = 3.2 Å) [26, 27]. The diffraction peaks at 26.88°/2θ (*d*₁₀₁ = 3.31 Å), 36.37°/2θ (*d*₁₁₀ = 2.47 Å), 43.5°/2θ (*d*₂₀₀ = 2.08 Å) and 68.59°/2θ (*d*₂₀₃ = 1.37 Å) are due to the reflections of quartz impurities, while the peak at 29.59°/2θ (*d*₁₀₄ = 3.032 Å) shows the presence of calcite [26, 27] (Fig. 1, curve 1). Other peaks at 15.65°/2θ (*d*₁₀₁ = 5.66 Å), 30.3°/2θ (*d*₁₁₃ = 2.95 Å), 52.62°/2θ (*d*₂₂₀ = 1.74 Å) and 18.3°/2θ (*d*₀₀₂ = 4.84 Å), 19.22°/2θ (*d*₁₁₀ = 4.61 Å) indicate the presence of alunite and gibbsite, respectively [26] (Fig. 1, curve 1).

In curve 2 (Fig. 1), the presence of 20°/2θ-diffraction peak shows the preservation of the tubular structure of Halloysite after treatment. This structure could improve the mineral catalytic effect. The decrease of peak intensities of quartz and the no-presence of calcite peaks in the diffractogram (Fig. 1, curve 2) explain the elimination of these minerals by acid treatment, which counteracts their inhibiting effect on catalytic reaction and improves the polymerization kinetic.

An increase of the characteristic peak intensity of 7Å-halloysite (12.11°/2θ) accompanied by a decrease of the peak intensity of 10 Å-halloysite (8.96°/2θ) were observed (Fig. 1, curve 2), which is due the dehydration of HAL-H⁺ during its drying at 40°C following the acid treatment [25, 27]. The no-shift of both halloysite peaks (001) to lower angles suggests no intercalation of sulfuric acid into interlayer space [26] (Fig. 1, curve 2), which maintains its structure. The acid treatment causes ionic exchange between H⁺ and interlayer cations associated with Al³⁺ of octahedral site which increase the clay acidity improving its catalytic activity [28, 29] without however affecting its crystalline

Table 2. Chemical composition (wt %), determined by FRX, of Halloysite (HAL)

Oxides	SiO ₂	Al ₂ O ₃	Fe ₂ O ₃	CaO	MgO	K ₂ O	Na ₂ O	L.O.I*
wt %	41.75	35.65	0.05	3.33	0.45	0.13	0.49	18.00

L.O.I*: Loss on ignition.

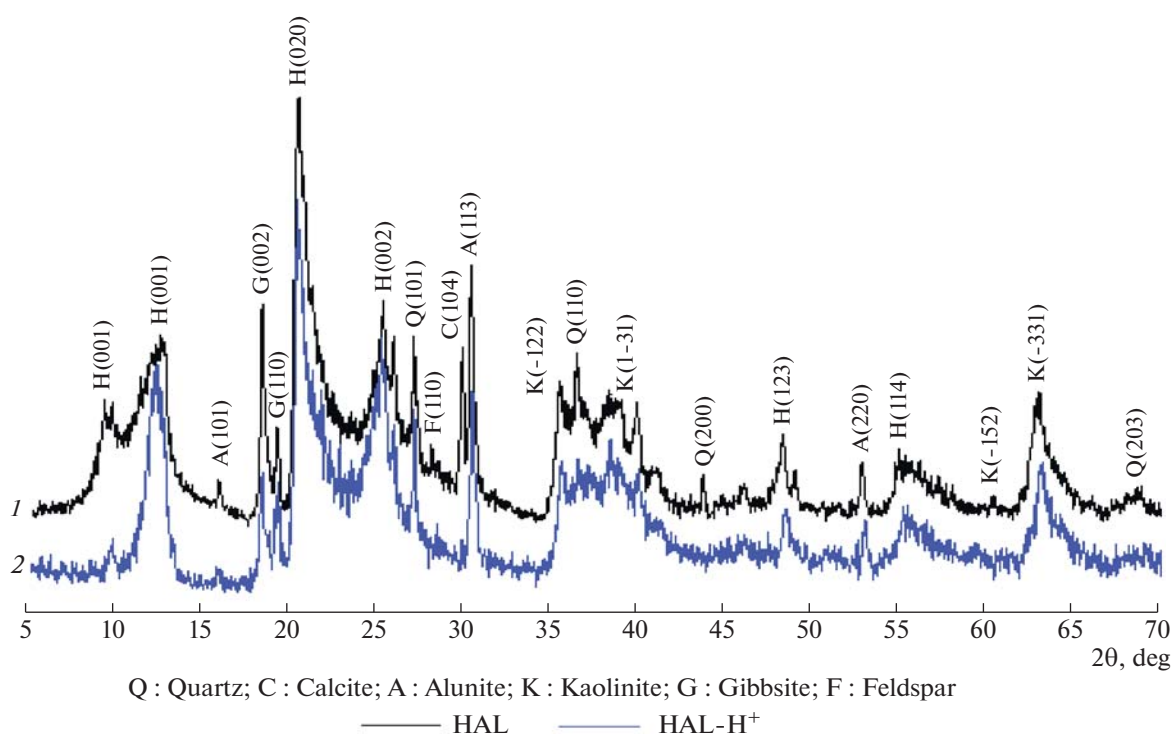


Fig. 1. XRD patterns of (1) natural halloysite (HAL) and (2) acid-activated halloysite (HAL-H⁺).

structure. These results show that a low concentration acid (0.5 M) does not affect the crystal structure of halloysite, which is different from a low pH sulfuric acid having a destructive effect on the mineral structure according to previous study [27].

FTIR spectroscopy characterization. The FTIR spectra of HAL and HAL-H⁺ samples are shown in Fig. 2. The double adsorption bands at 3693 and 3621 cm⁻¹ are ascribed to the stretching vibration of inner-surface OH groups and inner OH groups, respectively [30, 31]. The band at 1638 cm⁻¹ is due to bending vibrations of the OH group of adsorbed water in interlayer space. The 914 cm⁻¹ band assigns to the O–H deformation of inner Al–OH groups [32].

The shoulder at 1115 cm⁻¹ is attributed to stretching mode of apical Si–O, while the band at 1021 cm⁻¹ is associated to the stretching vibration of Si–O–Si. The bands at 793 and 749 cm⁻¹ are assigned to the stretching mode of Al–O–OH in the halloysite. The bands at 685 and 527 cm⁻¹ are caused by stretching vibration of Si–O–Al and Si–O–Al deformation, respectively [32].

No change was observed on the spectrum bands of HAL-H⁺ after halloysite acidification, indicating that acid-treatment has no influence on the structure of HAL, which is consistent with the XRD results.

Characterizations of the Synthesized Polymer (PDXL)

To confirm obtaining the desired polymer, poly(1,3-dioxolane), various characterizations were carried out: FTIR spectroscopy, ¹H NMR and ¹³C NMR analysis and XRD.

FTIR analysis. The monomer (DXL) and the obtained polymer (PDXL) were characterized by FTIR spectroscopy from 500 to 4000 cm⁻¹ wave number. The results are given by the spectra illustrated in Fig. 3.

The FTIR spectrum of the PDXL (Fig. 3, curve 2) exhibits two bands at 2952 and 2877 cm⁻¹ corresponding to methylene group. The same bands are present in the DXL spectrum at 2965 and 2886 cm⁻¹ (Fig. 3, curve 1). The new large band at 3483 cm⁻¹ is assigned to stretching vibration of hydroxyl group in the chain-end. The band at 1102 cm⁻¹ is attributed to C–O–C ether function [33]. The bands at 1016, 1241 and 1178 cm⁻¹ characterize the C–C and C–OH stretching vibration of polymer. The bands at 1468 and 1354 cm⁻¹ correspond to bending aliphatic C–H vibration, while the bands at 983 and 851 cm⁻¹ are attributed to the stretching vibration of aliphatic acetals. All these detected bands characterize the presence of the characteristic functional groups of the PDXL polymer.

¹H NMR and ¹³C NMR analysis. The nuclear magnetic resonance technique (NMR) was used to characterize the synthesized polymer. The ¹H NMR and

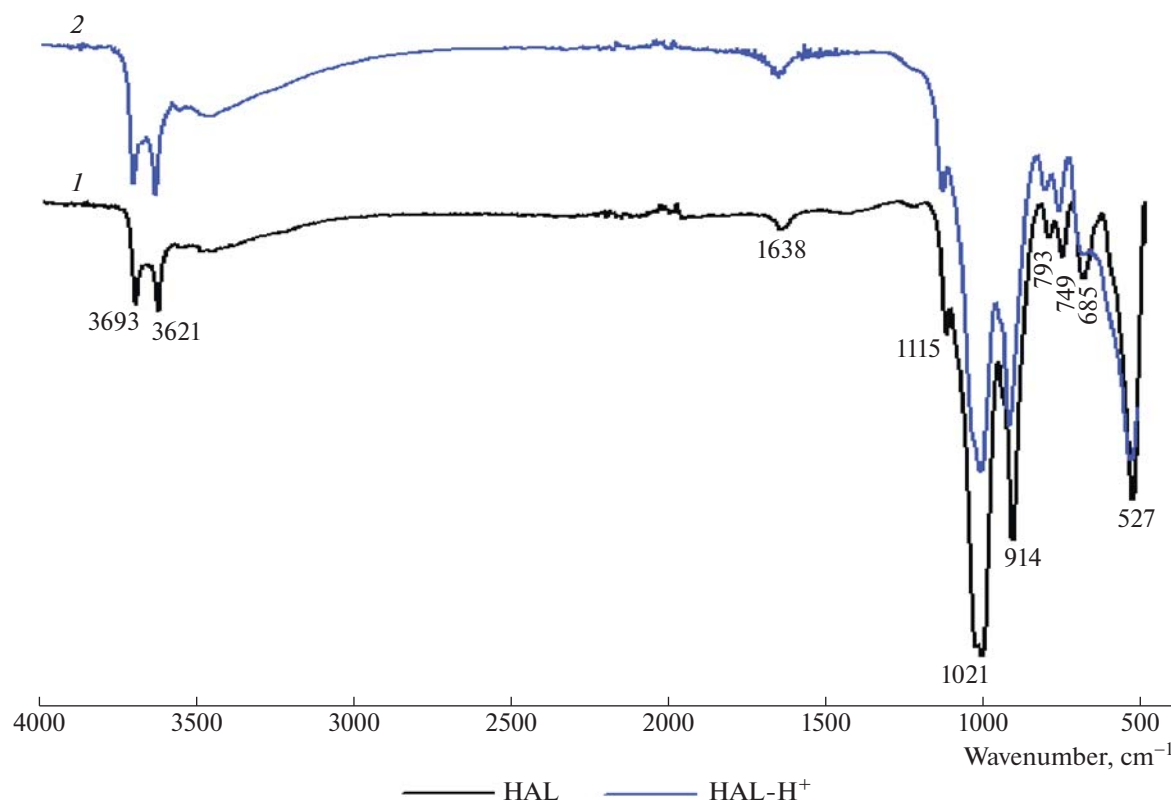


Fig. 2. FTIR spectra of (1) HAL and (2) HAL-H⁺.

¹³C NMR spectra of synthesized PDXL are shown in Figs. 4 and 5, respectively. In Fig. 4, the resonance signals observed at 3.60 ppm (b) and 4.639 ppm (a) are attributed to the $\text{—O—CH}_2\text{—CH}_2\text{—O—}$ and $\text{—O—CH}_2\text{—O—}$ protons in PDXL, respectively. The hydroxyl group protons of the chain-end (c) gave signal at $\delta_{\text{H}} = 2.5$ ppm (Fig. 4). In Fig. 5, the signals observed at 66.84 ppm (b) and 95.21 ppm (a) are assigned to the carbon groups $\text{—O—CH}_2\text{—CH}_2\text{—O—}$ and $\text{—O—CH}_2\text{—O—}$ of PDXL. According to other researches, the DXL characteristic peaks correspond to the same proton and carbon signals as found for the synthesized PDXL [34]. The peak at 40.16 ppm is attributed to DMSO- d_6 used for dissolving sample (Fig. 5). In addition, some residual peaks detected at $\delta_{\text{CH}} = 60.87$, 69.52, and 91.73 ppm (Fig. 5) can be attributed to DXL monomer [34].

It should be noted that ¹H NMR and ¹³C NMR spectra of the polymer (Figs. 4, 5) confirm the structure of PDXL.

Number-average molecular weight determination using proton NMR. The number-average molecular weight M_n was calculated by proton NMR from the integration of methylene protons of the $\text{—O—CH}_2\text{—CH}_2\text{—O—}$ group (Ib) and that of the hydroxyl protons of the chain ends as $M_n = 74n + 18 = 753.56$, where

$n = 9.94$ [23], n —the number of repeating monomer units.

X-ray diffraction characterization. To provide information about the structure nature of the synthesized polymer, the X-ray diffraction technique was used. The XRD pattern of polydioxolane (PDXL) is displayed in Fig. 6. The presence of only one characteristic peak of low intensity at $22^\circ/2\theta$ shows the quasi-amorphous structure of the synthesized PDXL. Similar result of pure PDXL confirming this structure was reported by Silva et al. [35].

Effect of PDXL Polymer on Normal Consistency and Setting Time of Cement Paste

The effect study of the polymer additive on the cement paste will characterize the change in its rheological properties. Cement pastes with the synthesized polymer (PDXL) and control polymer (PEG,) were mixed with a water-to-cement mass ratio (w/c) of 0.3. The solid form polymers were added separately to the mixing water with a mass percentage of 0.5% and 1.0% of cement weigh. The setting time and normal consistency of the cement paste, with and without polymer, were determined at ambient temperature ($20 \pm 1^\circ\text{C}$) using Vicat apparatus, according to NF EN 196-3 standard. The results of the normal consistency and setting times of cement pastes (initial and final), with

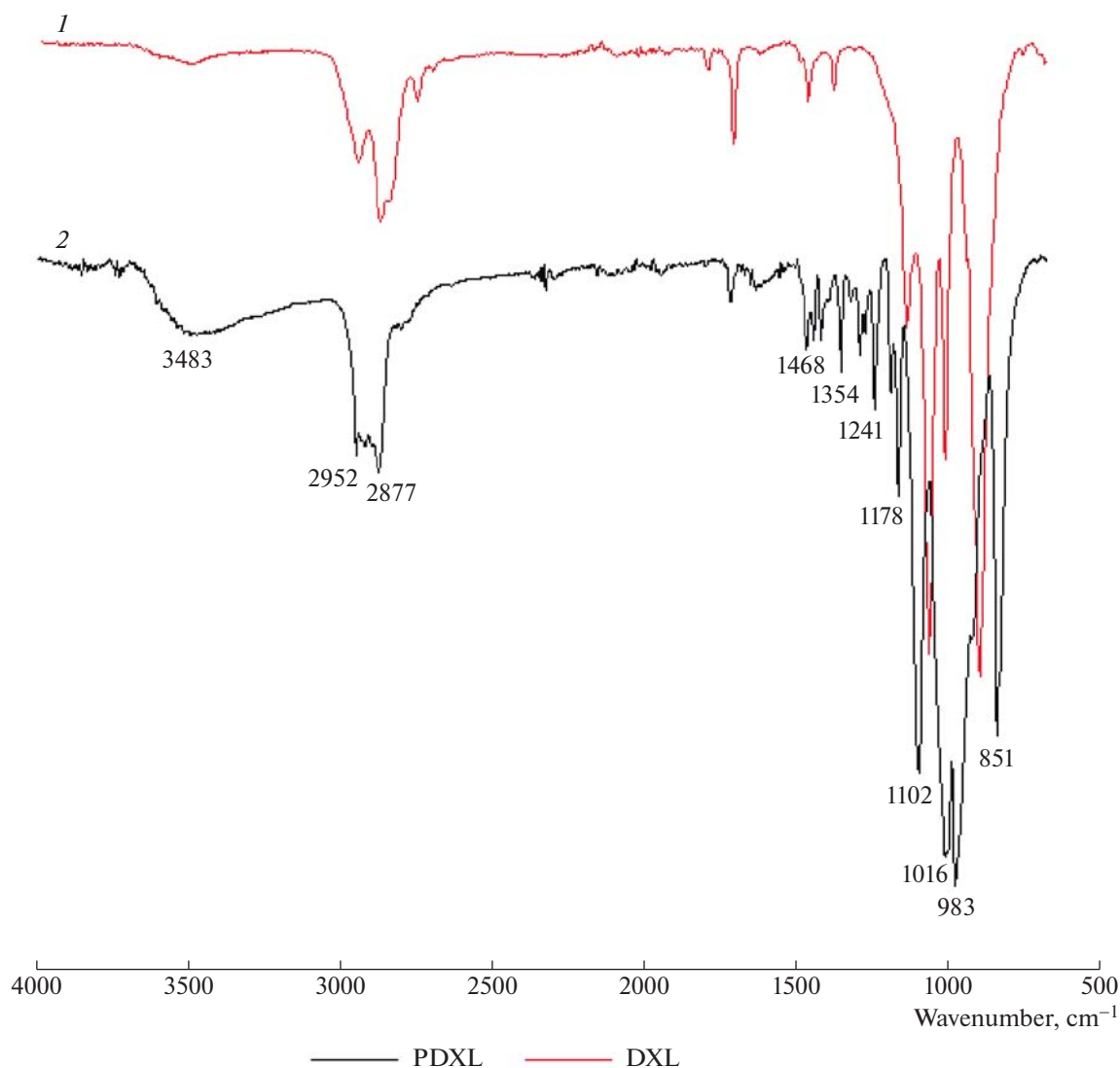


Fig. 3. FTIR spectra of (1) DXL monomer and (2) synthesized PDXL.

PDXL/PEG and without polymer are shown in Table 3 and Fig. 7, respectively.

An increase in the setting time of cement pastes (Fig. 7) accompanied with decrease of normal consistency values (Table 3) were observed by adding polymers. The polymer effect depends on its nature and its amount in the cement paste, of which the increase of PEG and PDXL percentage from 0.5 to 1.0% increased the initial and final setting times from (191 min; 256 min) to (235 min; 290 min) for PEG, and from (195 min; 260 min) to (240 min; 310 min) for

PDXL. The consistency decreases from 28.2 to 28.0 with adding PEG, and to 27.8 and 27.4 when 0.5 and 1% PDXL are added, respectively (Table 3). It was found that PDXL polymer extends the setting time and reduces the needed mixing water more than PEG.

The retarding effect of PDXL and PEG on cement paste setting is due to the dispersive effect of these polymers, which reduces the mixture viscosity. This was confirmed by the normal consistency results showing reducing the water amount needed for cement mixing (Table 3). Indeed, polydioxolane

Table 3. Normal consistency of cement pastes

Cement paste with	0% polymer	0.5% PEG	1.0% PEG	0.5% PDXL	1.0% PDXL
Consistency, wt %	28.2	28.0	28.0	27.8	27.4

The error interval from consistency measurement: $\pm 0.2\%$.

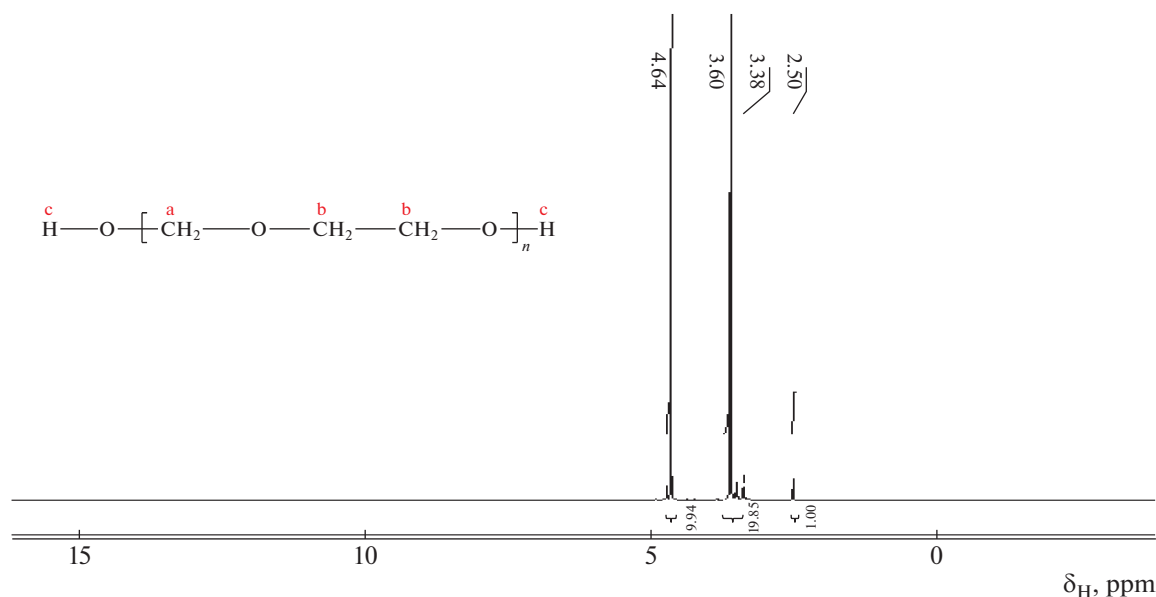


Fig. 4. ^1H NMR spectrum of PDXL in DMSO-d_6 .

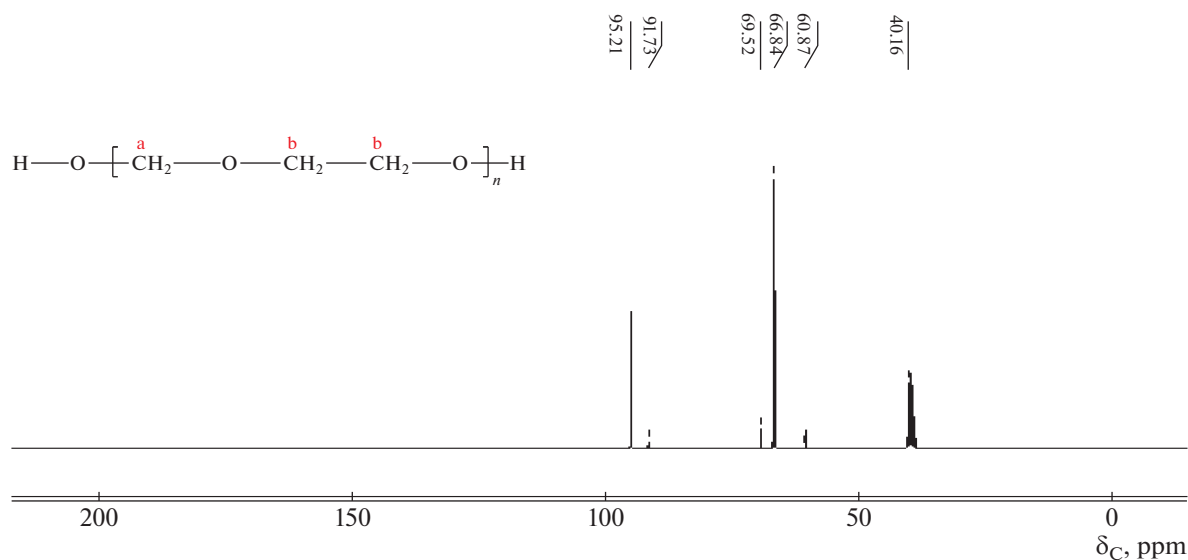


Fig. 5. ^{13}C NMR spectrum of PDXL in DMSO-d_6 .

(PDXL) and polyethylene glycol (PEG) are polyethers containing some ether bonds ($-\text{C}-\text{O}-\text{C}-$) in their polymer chains, in addition to hydrophilic hydroxyl functional groups at the chain-end. During hydration, the oxygen atoms of ether bonds and the water molecules form strong hydrogen bonds, producing an important hydrophilic steric protective barrier around the cement particles, which slows down their hydration and delays the paste setting [36]. Moreover, the polymerization of DXL, as all cyclic acetals, is subject to cyclization of the polymer linear chain, which conduces to the suspension dispersion by steric

hindrance. This explains the better dispersive power of PDXL comparing to PEG.

The normal consistency and setting time of cement paste are rheological indicators for the suspension which characterize its dispersive appearance. The results show that the addition of PDXL polymer allows increasing the suspension dispersion, and therefore lower its viscosity. This is a very important parameter to suggest this polymer as super-plasticizer in high-performance concretes (HPC) or as additive in petroleum cement slurry. It should be noted that the choosing optimum PDXL percentage is 0.5% because it

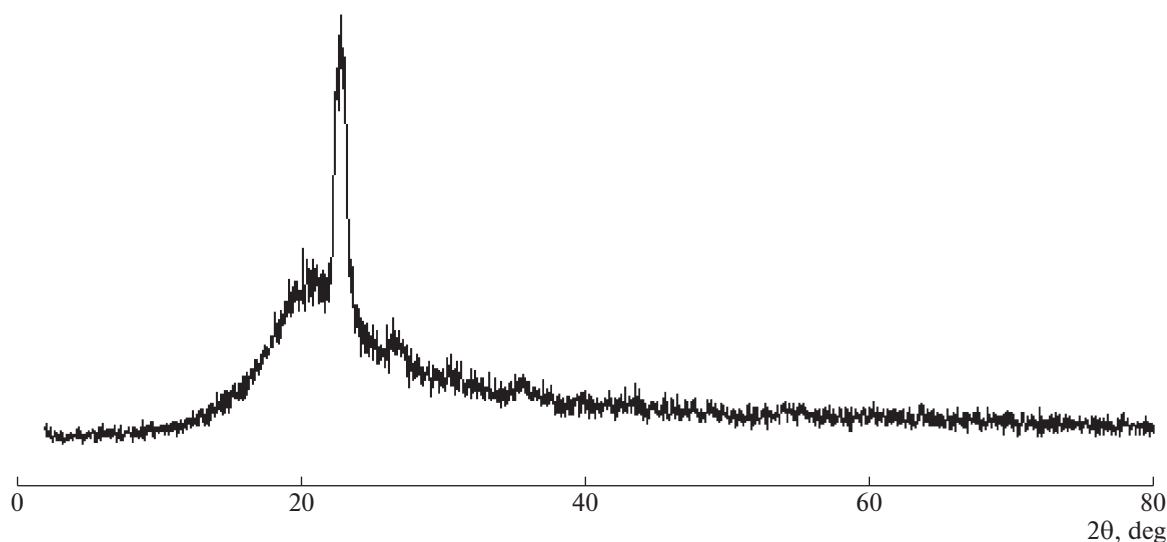


Fig. 6. X-ray diffractogram of PDXL.

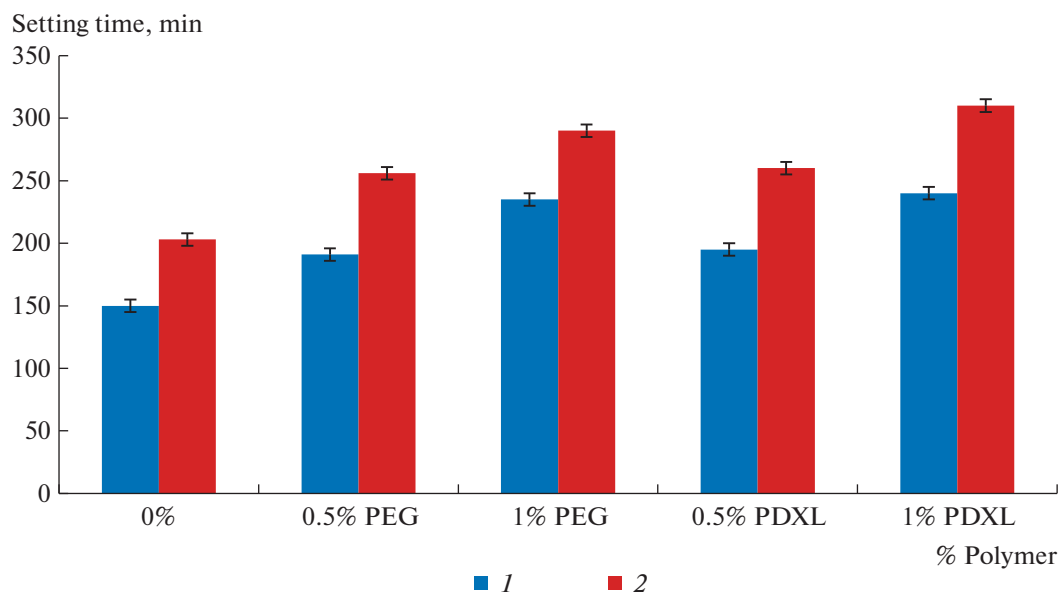


Fig. 7. Effect of PDXL on setting time of cement paste, compared to PEG effect: (1) initial setting, (2) final setting.

reduces the water demand without excessively prolonging the setting-end.

Effect of PDXL Polymer on Compressive Strength of Cement Mortar

The compressive strength results of cement mortars containing the control polymer (PEG) and the synthesized polymer (PDXL) are illustrated in Fig. 8.

The over time evolution of the compressive strength of mortars containing polymers is similar to that of mortars without additives, but with different values according to the polymer nature and amount

(Fig. 8). For any hardening age (2, 7, 28 days), the compressive strength values of mortars containing polymers were very important comparing to mortar without additive. They increase with increasing the added polymer amount, of which PDXL is more effective. At 28 days of hardening, mortar with PDXL presents 61.0 and 61.7 MPa for 0.5 and 1% of addition respectively. These high values, comparing to without and PEG polymer mortars, show the important effect of PDXL as superplasticizer which is probably due to a decrease of mortar porosity by reducing the mixing water amount, of which 0.5% was an optimum added amount. Water-soluble polymers are free of surfac-

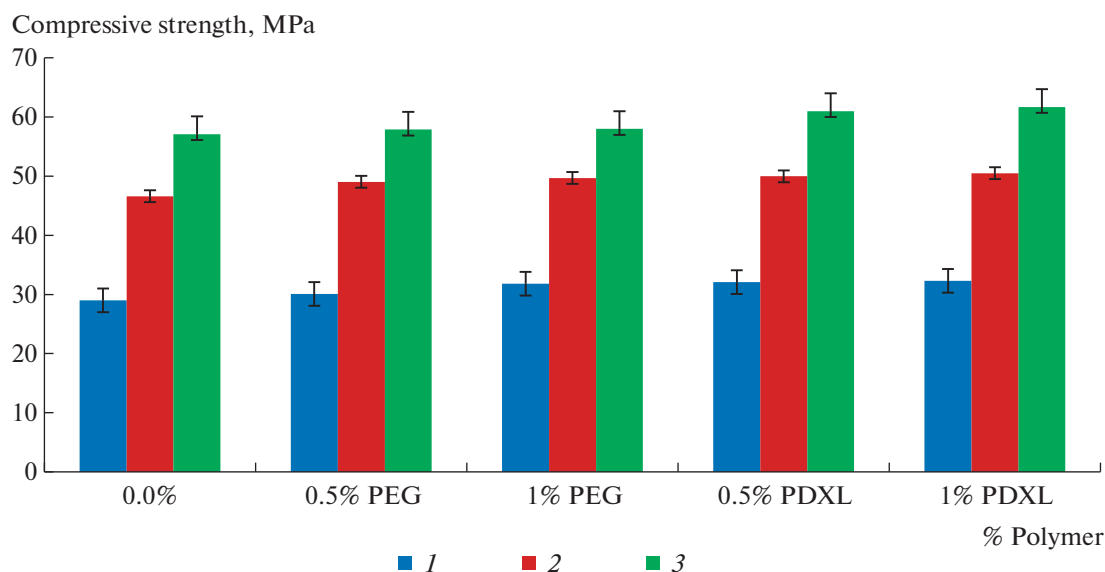


Fig. 8. Compressive strength of cement mortars with PEG/PDXL and without polymer: (1) 2, (2) 7, and (3) 28 days.

tants facilitating then the formation of polymer film around the cement particles during the hydration process. Increasing the polymer content will improve the protective effect of polymer, which improve the workability of fresh cement mortars by lowering its viscosity [37, 38]. According to Yuan et al. [39], the compressive strength of cement mortars increases with adding more polymer during the hardening process. This was in accordance with our results testifying the compressive strength improvement of mortars containing PDXL starting from 2 days of hardening.

CONCLUSIONS

A poly(1,3-dioxolane) was synthesized by cationic ring opening polymerization of 1,3-dioxolane, under heterogeneous conditions, using an Algerian halloysite clay. The activation of this no-expensive halloysite, very abundant in the Algerian earth's crust, and its use as eco-catalyst material represents the first originality of this work. The second originality is the PDXL synthesis and its application as superplasticizer or dispersant in cement paste.

The following conclusions should be taken into consideration:

—FTIR and $^1\text{H}/^{13}\text{C}$ NMR spectra confirmed obtaining PDXL polymer and identified its molecular structure.

—X-ray diffractogram shows the quasi-amorphous structure of the synthesized polymer.

—These results highlight the catalytic properties of halloysite in polymerization reactions of heterocyclic monomer.

—PDXL polymer decreased the normal consistency and increased the setting time of cement paste

more than PEG, tacked as control superplasticizer in this work. The water reducer and set-retardant effects increased with the polymer percentage, of which PDXL was more effective. This allows using this polymer (PDXL) as better super-plasticizer or dispersant agent in concrete or oil cement slurry with only 0.5%. However, a complementary study is necessary to assess the durability of cementitious materials containing this additive, as well as other required rheological parameters depending on the material use area.

FUNDING

This work was supported by ongoing institutional funding. No additional grants to carry out or direct this particular research were obtained.

CONFLICT OF INTEREST

The authors of this work declare that they have no conflicts of interest.

REFERENCES

1. S. Mohammadi and A. Babaei, *Int. J. Biol. Macromol.* **201**, 528 (2022).
2. M. Werani and L. Lei, *Constr. Build. Mater.* **281**, 122621 (2021).
3. E. J. Goethals, S. R. Walraedt, X. Han, G. G. Trossaert, and P. J. Hartmann, *Macromol. Symp.* **107**, 111 (1996).
4. Z. O. Elabed, D. E. Kherroub, H. Derdar, and M. Belbachir, *Polym. Sci., Ser. B* **63**, 480 (2021).
5. H. Derdar, M. Belbachir, F. Hennaoui, M. Akeb, and A. Harrane, *J. Polym. Sci., Ser. B* **60**, 555 (2018).

6. A. Moumen, Z. Hattab, Y. Belhocine, K. Guerfi, and N. Rebbani, *Bull. Chem. React. Eng. Catal.* **14**, 294 (2019).
7. R. Megherbi, M. Belbachir, and R. Meghabar, *J. Appl. Polym. Sci.* **101**, 78 (2006).
8. C. Bendiabdallah, F. Reguieg, and M. Belbachir, *Polym. Sci., Ser. B* **63**, 691 (2021).
9. S. Mellouk, S. Cherifi, M. Sassi, K. Marouf-Khelifa, A. Bengueddach, J. Schott, and A. Khelifa, *Appl. Clay Sci.* **44**, 230 (2009).
10. X. Tian, W. Wang, N. Tian, C. Zhou, C. Yang, and S. Komarneni, *J. Hazard. Mater.* **309**, 151 (2016).
11. R. C. Liu, B. Zhang, D. D. Mei, H. Q. Zhang, and J. D. Liu, *Desalination* **268**, 111 (2011).
12. R. Riahi-Madvaar, M. A. Taher, and H. Fazelirad, *Appl. Clay Sci.* **137**, 101 (2017).
13. L. Zatta, J. E. F. da Costa Gardolinski, and F. Wypych, *Appl. Clay Sci.* **51**, 165 (2011).
14. N. Sabbagh, A. Akbari, N. Arsalani, B. Eftekhari-Sis, and H. Hamishekar, *Appl. Clay Sci.* **148**, 48 (2017).
15. S. Sharif, G. Abbas, M. Hanif, A. Bernkop-Schnürch, A. Jalil, and M. Yaqoob, *Colloids Surf., B* **184**, 110527 (2019).
16. K. Buruga and J. T. Kalathi, *J. Alloys Compd.* **735**, 1807 (2018).
17. H. G. Hester, B. A. Abel, and G. W. Coates, *J. Am. Chem. Soc.* **145**, 8800 (2023).
18. P. J. Lutz, *Polym. Bull.* **58**, 161 (2007).
19. F. Reguieg, N. Sahli, and M. Belbachir, *Orient. J. Chem.* **31**, 1645 (2015).
20. Y. Nakajimaa and K. Yamada, *Cem. Concr. Res.* **34**, 839 (2004).
21. Q. H. Zhu, L. Z. Zhang, X. M. Min, Y. X. Yu, X. F. Zhao, and J. H. Li, *Colloids Surf., A* **553**, 272 (2018).
22. W. Fan, F. Stoffelbach, J. Rieger, L. Regnaud, A. Vichot, B. Bresson, and N. Lequeux, *Cem. Concr. Res.* **42**, 166 (2012).
23. N. Ouis, N. Benharrats, and M. Belbachir, *C. R. Chim.* **7**, 955 (2004).
24. Y. Li, Y. Zhang, Y. Zhang, M. Liu, F. Zhang, and L. Wang, *J. Therm. Anal. Calorim.* **129**, 1333 (2017).
25. A. B. Zhang, L. Pan, H. Y. Zhang, S. T. Liu, Y. Ye, M. S. Xia, and X. G. Chen, *Colloids Surf., A* **396**, 182 (2012).
26. J. M. Falcón, T. Sawczen, and I. V. Aoki, *Front. Mater.* **2**, 4464 (2015).
27. E. Joussein, S. Petit, J. Churchman, B. Theng, D. Righi, and B. Delvaux, *Clay Miner.* **40**, 383 (2005).
28. E. Abdullayev, A. Joshi, W. Wei, Y. Zhao, and Yu. Lvov, *ACS Nano* **6**, 7216 (2012).
29. A. R. Nascimento, J. A. Alves, M. A. Melo, D. M. Melo, M. J. Souza, and A. M. Pedrosa, *Mater. Res.* **18**, 283 (2015).
30. H. Cheng, Q. Liu, J. Yang, J. Zhang, and R. L. Frost, *Thermochim. Acta* **511**, 124 (2010).
31. R. L. Frost, J. Kristof, E. Horvath, and J. T. Klopogge, *J. Colloid Interface Sci.* **226**, 318 (2000).
32. Y. Zhang, Y. Li, and Y. Zhang, *Appl. Clay Sci.* **187**, 105451 (2020).
33. W. Zhu, X. L. Wang, B. Yang, L. Wang, X. Z. Tang, and C. Yang, *J. Mater. Sci.* **36**, 5137 (2001).
34. J. M. Williams, H. R. Schulten, N. E. Vanderborgh, and R. D. Walker, *Polymer* **33**, 4630 (1992).
35. R. A. Silva, G. G. Silva, C. A. Furtado, R. L. Moreira, and M. A. Pimenta, *Electrochim. Acta* **46**, 1493 (2001).
36. E. Sakai, K. Yamada, and A. Ohta, *J. Adv. Concr. Technol.* **1**, 16 (2003).
37. E. Knapen, and D. Van Gemert, *Cem. Concr. Compos.* **58**, 23 (2015).
38. E. Knapen, PhD Thesis (KU Leuven, Belgium, 2007).
39. Q. Yuan, Z. Xie, H. Yao, T. Huang, and M. Fan, *J. Build. Eng.* **56**, 104763 (2022).

Publisher's Note. Pleiades Publishing remains neutral with regard to jurisdictional claims in published maps and institutional affiliations. AI tools may have been used in the translation or editing of this article.